

See discussions, stats, and author profiles for this publication at: <https://www.researchgate.net/publication/5636715>

# The insecticidal protein hirsutellin A from the mite fungal pathogen *Hirsutella thompsonii* is a ribotoxin

ARTICLE *in* PROTEINS STRUCTURE FUNCTION AND BIOINFORMATICS · JULY 2008

Impact Factor: 2.63 · DOI: 10.1002/prot.21910 · Source: PubMed

---

CITATIONS

18

---

READS

48

7 AUTHORS, INCLUDING:



**Elías Herrero-Galán**

Spanish National Research Council

16 PUBLICATIONS 198 CITATIONS

SEE PROFILE



**Alvaro Martínez-del-Pozo**

Complutense University of Madrid

146 PUBLICATIONS 2,528 CITATIONS

SEE PROFILE



**Drion Boucias**

University of Florida

203 PUBLICATIONS 2,853 CITATIONS

SEE PROFILE

# The insecticidal protein hirsutellin A from the mite fungal pathogen *Hirsutella thompsonii* is a ribotoxin

Elías Herrero-Galán,<sup>1</sup> Javier Lacadena,<sup>1</sup> Álvaro Martínez del Pozo,<sup>1</sup> Drion G. Boucias,<sup>2</sup> Nieves Olmo,<sup>1</sup> Mercedes Oñaderra,<sup>1\*</sup> and José G. Gavilanes<sup>1\*</sup>

<sup>1</sup> Departamento de Bioquímica y Biología Molecular I, Universidad Complutense, 28040 Madrid, Spain

<sup>2</sup> Department of Entomology and Nematology, University of Florida, Florida

## ABSTRACT

The mite fungal pathogen *Hirsutella thompsonii* produces a single polypeptide chain, insecticidal protein named hirsutellin A (HtA) that is composed of 130 amino acid residues. This protein has been purified from its natural source and produced as a recombinant protein in *Escherichia coli*. Spectroscopic analysis has determined that the two protein forms are indistinguishable. HtA specifically inactivates ribosomes and produces the  $\alpha$ -fragment characteristic of ribotoxin activity on rRNA. Behaving as a cyclizing ribonuclease, HtA specifically cleaves oligonucleotides that mimic the sarcin/ricin loop of the ribosome, as well as selected polynucleotides and dinucleosides. HtA interacts with phospholipid membranes as do other ribotoxins. As a consequence of its ribonuclease activity and its ability to interact with cell membranes, HtA exhibits cytotoxic activity on human tumor cells. On the basis of these results, HtA is considered to be a member of the ribotoxin group of proteins, although it is significantly smaller (130 aa) than all known ribotoxins that are composed of 149/150 amino acids. Ribotoxins are members of a larger family of fungal ribonucleases whose members of smaller size (100/110 aa) are not cytotoxic. Thus, the characterization of the fungal ribotoxin HtA represents an important milestone in the study of the diversity and the function of fungal ribonucleases.

Proteins 2008; 72:217–228.  
© 2008 Wiley-Liss, Inc.

**Key words:** cytotoxic protein; restrictocin; ribonuclease; ribosome; RNase T1;  $\alpha$ -sarcin.

## INTRODUCTION

Ribotoxins are a family of ribosome-inactivating proteins displaying specific ribonucleolytic activity against a single phosphodiester bond at the universally conserved sarcin/ricin loop (SRL) of the 28S ribosomal RNA.<sup>1–4</sup> Cleavage of this phosphodiester bond impairs ribosome function, resulting in cell death.<sup>5,6</sup>  $\alpha$ -Sarcin, from *Aspergillus giganteus*, and restrictocin, from *A. restrictus*, are the best-characterized members, although other ribotoxins have been isolated from different *Aspergillus* strains (clavin, gigantin, c-sarcin, Aspf 1).<sup>7–10</sup> All known ribotoxins are single-polypeptide chain (~17 kDa) basic proteins displaying a highly conservative primary structure<sup>4,11,12</sup> (Fig. 1). The three-dimensional structures of  $\alpha$ -sarcin and restrictocin are similar<sup>14–16</sup>; they share properties with nontoxic ribonucleases of the RNase T1 family (Fig. 1). Besides the overall protein fold, similarities include the nature and location of the catalytic residues as well as the enzymatic mechanism.<sup>17,18</sup> The main structural differences between ribotoxins and nontoxic RNases are the length and arrangement of the nonordered protein loops, believed to be responsible for the cytotoxic character of ribotoxins.<sup>19,20</sup> Their ability to enter cells and to display specific ribonucleolytic action against a single phosphodiester bond in the whole ribosome could have evolved from the characteristic properties displayed by the family of the nontoxic fungal ribonucleases.

Hirsutellin A (HtA) is an extracellular protein produced by the invertebrate fungal pathogen *Hirsutella thompsonii*, and some of its biological properties resemble those of the ribotoxin family.<sup>21</sup> Alignment of the primary structure deduced from the HtA cDNA sequence<sup>22</sup> with those of ribotoxins revealed a significant similarity.<sup>12</sup> Sequence identity between HtA and ribotoxins was only about 25%, a value much less than that among known ribotoxins (always above 60%). Significantly, the sequence conservation between HtA and ribotoxins included the catalytic residues (Fig. 1). Interestingly, HtA is 20 residues shorter than  $\alpha$ -sarcin-type proteins. The deletion of amino acids would presumably be located at the

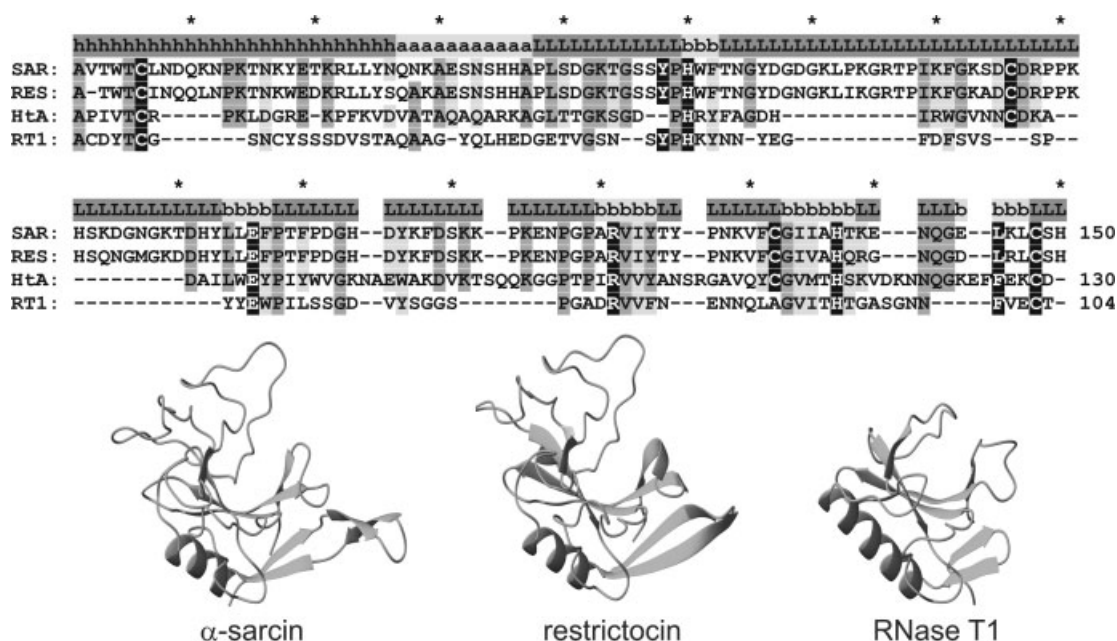
\*Correspondence to: Mercedes Oñaderra or José G. Gavilanes, Departamento de Bioquímica y Biología Molecular, Facultad de Química, Universidad Complutense, 28040 Madrid, Spain.  
E-mail: mos@bbm1.ucm.es or ppfg@bbm1.ucm.es.

Grant sponsor: Ministerio de Educación y Ciencia, Spain; Grant number: BFU2006-04404.

Received 26 June 2007; Revised 27 September 2007; Accepted 31 October 2007

Published online 23 January 2008 in Wiley InterScience (www.interscience.wiley.com).

DOI: 10.1002/prot.21910

**Figure 1**

Alignment of the amino acid sequences of  $\alpha$ -sarcin (SAR), restrictocin (RES), hirsutellin A (HtA), and RNase T1 (RT1). Conserved residues (grey boxes) and conservative substitutions (light grey boxes) in at least three sequences are enlightened, as well as the cysteine residues and catalytic residues of ribotoxins (black boxes). (h) Stands for residues corresponding to the  $\text{NH}_2$ -terminal  $\beta$ -hairpin, (a) residues at the helical portion, (b) residues in  $\beta$ -strands, and (L) residues in loops of  $\alpha$ -sarcin. (\*) Marks at each 10 residues of  $\alpha$ -sarcin. The three-dimensional structures of  $\alpha$ -sarcin, restrictocin, and RNase T1 are also shown. Images were generated with the MOLMOL program<sup>13</sup> from the atomic coordinates deposited in PDB (entries: 1DE3, 1AQZ, 1RNT, for  $\alpha$ -sarcin, restrictocin, and RNase T1, respectively). The structures were fitted according to the coordinates of the peptide bond atoms of residues 6, 48, 50, 96, 121, 137, 145, and 148 (numbering of  $\alpha$ -sarcin; residues 6 and 148 correspond to the disulfide bridge common to ribotoxins and nontoxic ribonucleases; the other residues are involved in the catalysis of both families of proteins; RMSD of the fitting: 0.461).

protein loops, which are considered to be essential for some of the specific activities of ribotoxins (Fig. 1).<sup>23,24</sup> We speculate that HtA is a protein related to both ribotoxins and to smaller, nontoxic fungal ribonucleases. The aims of this study are to characterize natural and recombinant HtA proteins and to analyze their ribotoxin characteristics to further our understanding of the natural diversity and biological function of the  $\alpha$ -sarcin family proteins.

## MATERIALS AND METHODS

### Recombinant DNA manipulations

All materials and reagents were of molecular biology grade. A clone of the HtA cDNA was obtained previously.<sup>22</sup> Tac-tac HtA (Fig. 2), the plasmid for the expression of mature HtA in *E. coli*, was constructed as follows. Two oligonucleotides were used to amplify the HtA cDNA by PCR to incorporate the recognition sequences for *Nde*I and *Eco*RI at both the initiation Met residue and the stop codons, respectively. Primer 1 (upstream primer with *Nde*I site) was 5'-GTGACACCATATGGCTCCATCGTCACCTGCCGCCCA-3' and primer 2 (return primer with *Eco*RI site) was 5'-CTTTGAGAAGTGCGATTAGATGGAATTC-3'. Primers were synthesized by Sigma

Genosys. PCR procedures were carried out at 55°C, for 30 cycles following standard methods.<sup>3</sup> A fragment of about 400 bp containing the mature HtA cDNA obtained after amplification and digestion with *Nde*I and *Eco*RI was subcloned into TOPO vector (Promega). The identity of the insert in the TOPO-HtA plasmid was confirmed by automatic sequencing and double digestion with both restriction enzymes. This excision fragment of DNA was ligated into the corresponding sites of the tailor-made vector poly-His-pCWori-SR plasmid.<sup>25,26</sup> This construct, designated as tac-tac HtA, was used for the production and purification of the 6His-tagged recombinant protein. All cloning procedures and enzymatic reactions were carried out as described<sup>27,28</sup> following standard procedures.<sup>29</sup> HtA insert in the plasmid was verified by sequence analysis.

### Protein production and purification

*E. coli* BL21 (DE3) cells harboring the HtA plasmid were grown in 4 L of LB medium, containing 100  $\mu\text{g}/\text{mL}$  ampicillin until an  $\text{OD}_{600}$  of 0.8 was reached. Cultures were induced with 1 mM IPTG and cultured at 37°C under vigorous shaking for an additional 4 h. Cells pelleted by centrifugation were suspended in 200 mL of sonication buffer (100 mM Tris, 0.3M NaCl buffer, pH 7.8,

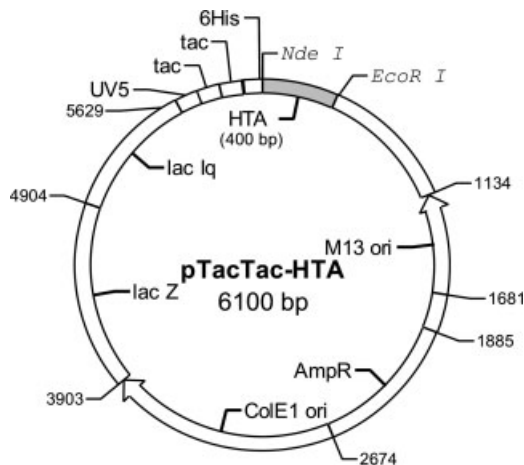


**Figure 2**

Construct plasmid for HtA expression (*tac-tac-HtA* plasmid). AmpR, ampicillin resistance gene; colE1 ori, *E. coli* replication origin; M13 ori, phage M13 replication origin; NdeI and EcoRI, the restriction sites used to insert the HTA cDNA sequence; (*lacZ*, *lacIq*, UV5, *tac*, *tac*), promoter cassette. The position of the 6 His-tag is also indicated.

1% (v/v) Tween 20), sonicated on ice (five pulses of 0.5 min at 20 Kc), and centrifuged at 14,000g for 20 min at 4°C. The supernatant was mixed with 1.5 mL of Ni<sup>2+</sup>-nitrilotriacetic acid agarose (low %Ni<sup>2+</sup>, 5–20 µmol Ni/mL gel; Agarose Bead Technologies), gently shaken for 1 h at 4°C, and loaded onto a chromatographic column. This column was sequentially washed with sonication buffer and then with 10 mM MOPS buffer, pH 7.8, containing 30 mM imidazole. The 6His-tagged HtA (6H-HtA) was eluted with 10 mM MOPS buffer, pH 7.8, containing 200 mM imidazole. Fungal wild-type HtA was obtained from broth cultures of *Hirsutella thompsonii* var. *thompsonii* HTF72 (Centraalbureau voor Schimmelfcultures, CBS952.73).<sup>30,31</sup> In this case, protein purification included running the sample through two ion-exchange columns, first on DEAE-cellulose (DE52 Whatman), equilibrated in 50 mM Tris, pH 8.0, and then on CM-cellulose (CM52 Whatman), equilibrated in 50 mM sodium acetate, pH 5.0, containing 0.1M NaCl. The protein was eluted from the second column with a 600-mL linear gradient (0.25–0.4M NaCl in the same buffer). Polyacrylamide gel electrophoresis, protein hydrolysis, and amino acid analysis were performed according to standard procedures.<sup>27</sup> Western blots were developed by using a mouse monoclonal antiserum raised against natural HtA<sup>30</sup> and against anti-6-His antibodies.

### Structural characterization

The spectroscopic characterization was performed using well-established procedures.<sup>3,10,18,23,24</sup> Absorbance measurements were performed on a Beckman DU640 spectrophotometer at 100 nm/min scanning

speed at room temperature and in 1-cm optical path cells. Circular dichroism (CD) spectra were obtained on a Jasco 715 spectropolarimeter, equipped with a thermostated cell holder and a NesLab-111 circulating water bath, at 0.2 nm/s scanning speed. The instrument was calibrated with (+)-10-camphorsulfonic acid. CD spectra were recorded in cylindrical cells of 0.1 or 1.0 cm optical path. Mean residue weight ellipticities were expressed in units of degree × cm<sup>2</sup> × dmol<sup>-1</sup>. Thermal denaturation profiles were obtained by measuring the temperature dependence of the ellipticity at 215 nm in the 25–85°C range; the temperature was continuously changed at a rate of 0.5°C/min. Fluorescence emission spectra were recorded on a SLM Aminco 6000 spectrofluorimeter at 25°C using 4-nm slits for both excitation and emission beams. The spectra were recorded for excitation at both 275 and 295 nm. Temperature was controlled by a circulating water bath. Thermostated cells of 0.2- and 1.0-cm optical paths for the excitation and emission beams, respectively, were used.

Differential scanning calorimetry (DSC) analysis of the protein was performed on a VP-DSC Microcal at 30°C/h speed, as described.<sup>32</sup>

### Ribonucleolytic activity

The specific ribonucleolytic activity of HtA on ribosomes was assayed by detecting the release of the 400 nt α-fragment from ribosomes contained in a rabbit cell-free reticulocyte lysate. This α-fragment was visualized by ethidium bromide staining after electrophoresis on denaturing 2.4% agarose gels.<sup>27,33</sup> The specific cleavage by HtA of an SRL-like synthetic 35mer RNA was also measured. The synthesis of this SRL RNA was performed as described.<sup>33</sup> The assay was performed with 2 µM SRL RNA and incubation was done for 15 min at 37°C in 40 mM Tris-HCl buffer, pH 7.5, containing 10 mM EDTA and 40 mM KCl. The reaction products were detected by ethidium bromide staining after electrophoretic separation on a denaturing 19% (w/v)-polyacrylamide gel. The specific action of HtA produced both 21mer and 14mer fragments. In addition, the activity of the purified proteins against *Torula* yeast RNA and homopolynucleotides (zymogram) was also studied. Volumograms of the electrophoretic bands (based on integrating all of the pixel intensities composing each spot) were obtained with the gel photodocumentation system (UVItec) and the software facility UVIsoft UVI band Windows Application V97.04. These data were used to quantify the enzyme activity on the different assays. Moreover, enzymatic hydrolyses of different dinucleoside phosphates at pH 7.0 were also performed as described before,<sup>17</sup> and reaction products were fractionated and quantified by HPLC. All these enzymatic assays including appropriate control reactions were performed as previously described.<sup>4,33</sup> Nonspecific degradation of target substrates did not occur in control assays.



## Phospholipid vesicle assays

All of the phospholipids used were purchased from Avanti Polar Lipids. Vesicles were formed by hydrating a dry lipid film with 15 mM Tris, pH 7.0, containing 0.1M NaCl and 1 mM EDTA, for 60 min at 37°C. This lipid suspension was then subjected to five cycles of extrusion through two stacked 0.1  $\mu$ m (pore diameter) polycarbonate membranes.<sup>3,34</sup> The average diameter of the vesicle population was 100 nm (85% of the vesicles in the range 75–125 nm), as determined by electron microscopy studies.<sup>34</sup> Phospholipid concentration was determined as described.<sup>35</sup> Aggregation was monitored as described before<sup>36</sup> by measuring the increase of the absorbance at 360 nm of a suspension of vesicles (30  $\mu$ M final lipid concentration) after addition of a small aliquot of a freshly prepared solution of protein. Leakage of vesicle aqueous contents was measured by using the 8-aminonaphthalene-1,3,6-trisulfonic acid/*N,N*-*p*-xylene-bispyridinium bromide assay as previously described.<sup>37</sup> All assays were performed after addition of a small aliquot of a freshly prepared solution of protein in the corresponding buffer. Other experimental details were as previously reported.<sup>34,38–43</sup>

## Cytotoxicity assay

This assay was performed essentially as described<sup>5,6</sup> by using human rhabdomyosarcoma cells. Protein synthesis was followed by measuring the incorporation of L-[4, 5-<sup>3</sup>H] leucine (166 Ci/mmol). Radioactivity was measured on a Beckman LS 3801 liquid scintillation counter. Results were expressed as percentages of radioactivity incorporation in control samples. Percentage values were plotted against protein concentration to calculate IC<sub>50</sub> values (protein concentration inhibiting 50% protein synthesis) in the cytotoxicity assays. Three replicate assays were conducted to calculate the average IC<sub>50</sub> values.

# RESULTS

## Cloning, expression, and purification of recombinant HtA

The expression plasmid designated as tac-tac HtA (Fig. 2) was used for the production of 6H-HtA. This plasmid is a tailor-made construction derived from the pCWori plasmid.<sup>25,26</sup> pCWori leads to a constant synthesis of the desired polypeptide that allows the *E. coli* machinery to keep up with other cellular functions.<sup>26</sup> Thus, it is a suitable vector for the recombinant expression of cytotoxic proteins in *E. coli*. Constructions using other plasmids used to produce  $\alpha$ -sarcin<sup>27</sup> did not yield satisfactory levels of recombinant HtA. Different cells were tested for optimal protein production. The highest yield was obtained with BL21(DE3) *E. coli*. Different culture conditions were also tested, and induction with 1 mM

IPTG, at 37°C for 4 h, resulted in maximal expression of functional HtA as determined by SDS-PAGE and activity assays. The BL21(DE3) cells containing the protein were also suspended and further disrupted in different buffers. Sonication in 50 mM Tris buffer, pH 7.8, containing 0.3M NaCl and 1% (v/v) Tween 20 rendered the highest levels of soluble recombinant protein. Purification using a Ni-NTA (low % Ni) affinity column provided a homogeneous preparation of 6H-HtA that eluted with 10 mM MOPS buffer, pH 7.8, containing 200 mM imidazol. This procedure yielded ~1 mg of purified protein/litre of culture. The recombinant protein immunoreacted with both anti-HtA and anti 6-His antibodies in Western blots (data not shown).

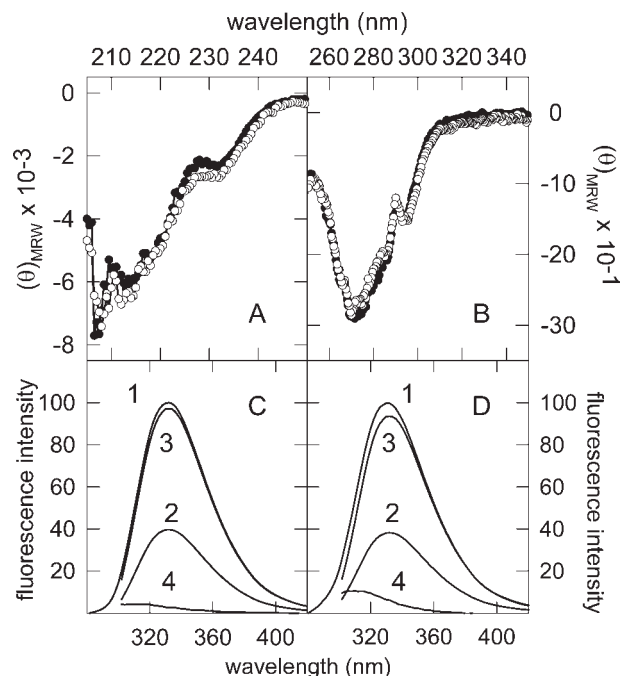
## Structural characterization of fungal and recombinant HtA

The amino acid composition of both natural and recombinant purified protein HtA agreed with the expected values,<sup>22</sup> including the presence of the seven extra amino acids (6His-tag and Met) at the NH<sub>2</sub> terminal end of the recombinant protein. Neither the purified natural nor the recombinant HtA contained free sulfhydryl groups as deduced from the absence of any absorbance increase at 412 nm upon treatment of the proteins with 5,5'-dithio-bis-nitrobenzoate in the presence of 5M guanidinium hydrochloride. Absorption spectra and amino acid analyses were used to calculate the extinction coefficients of both proteins. The experimentally determined *E* values (0.1%, 280 nm, 1 cm) were 2.05 for recombinant HtA and 2.00 for the fungal protein, and were within 5% of the value predicted from their amino acid composition.<sup>44</sup>

The far-UV CD spectra demonstrated that the secondary structure of both natural and recombinant HtA were coincident [Fig. 3(A)]. Convex constraint analysis<sup>45</sup> of the far-UV CD spectrum revealed that the secondary structure of HtA in solution would be composed of 16%  $\alpha$ -helix, 47%  $\beta$ -structure plus  $\beta$ -turns, and 37% nonregular conformation. Natural and recombinant HtA also displayed indistinguishable dichroism spectra in the near-UV regions [Fig. 3(B)] as well as fluorescence emission spectra for excitation at both 275 and 295 nm [Fig. 3(C,D)]. From these results, it was concluded that tertiary structure relationships involving the aromatic residues (near-UV CD and fluorescence emission spectra) for both fungal and recombinant HtA were essentially identical, revealing that the 6-His extra region did not modify the conformation of the protein.

## Thermal denaturation

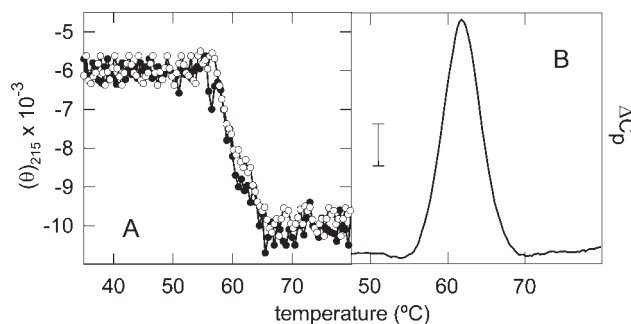
The thermal denaturation profile obtained by recording the ellipticity at 215 nm [Fig. 4(A)] was consistent with a two-state process and agreed with a folded–

**Figure 3**

Circular dichroism spectra in the (A) far-UV and (B) near-UV region of natural (filled circles) and recombinant (empty circles) hirsutellin A.  $(\theta)_{MRW}$  mean residue weight ellipticity in units of degree  $\times$  cm<sup>2</sup>  $\times$  dmole<sup>-1</sup>. Fluorescence emission spectra of fungal (C) and recombinant (D) for excitation at (1) 275 nm and (2) 295 nm; (3) emission spectra for excitation at 295 nm and further normalization at wavelengths above 380 nm where the contribution of tyrosine is negligible; (4) difference spectrum (1 - 3). Tryptophan and tyrosine emission are given by spectra 3 and 4, respectively. The spectra were recorded at 25°C. Fluorescence emission is expressed in arbitrary units.

unfolded transition. This transition was fully reversible because the far-UV CD spectrum obtained after cooling down the system corresponded to the native protein. The  $T_m$  value for HtA was 62°C,  $T_m$  value being the temperature at the midpoint of the observed single phase thermal transition. This value was 10°C higher than that reported for  $\alpha$ -sarcin<sup>41</sup> but closer to 61 and 59°C, the  $T_m$  value for the ribotoxins Aspfl and restrictocin, respectively.<sup>10,23</sup> The enthalpy change calculated from this experiment was 93 kcal/mol (Table I). The thermal denaturation profiles of fungal and recombinant HtA proteins supported our contention that both proteins were similarly folded.

The DSC curve obtained for the thermal unfolding of fungal HtA is shown in Figure 4(B). This thermogram exhibited a single and highly symmetrical peak, centered at 61.8°C, corresponding to the thermal unfolding of the protein. In this case, the  $\Delta H_{cal}$  value determined for the fungal protein from DSC measurements was 85 kcal/mol (Table I). Again, it confirmed the thermal unfolding reversibility, as demonstrated by the consistency of the thermograms obtained after several cycles of heating-cooling.

**Figure 4**

(A) Thermal denaturation profiles of fungal (solid circles) and recombinant HtA (open circles). Measurements were performed by continuously recording the ellipticity at 215 nm,  $(\theta)_{215}$  (in units of degree  $\times$  cm<sup>2</sup>  $\times$  dmole<sup>-1</sup>), upon temperature increase. The scan rate was 0.5°C/min. (B) Excess heat capacity ( $\Delta C_p$ ) of HtA versus temperature (°C). The scan rate was 30°C/h. Bar represents a heat capacity of 2 kcal K<sup>-1</sup> mol<sup>-1</sup>.

### Functional characterization of fungal and recombinant HtA

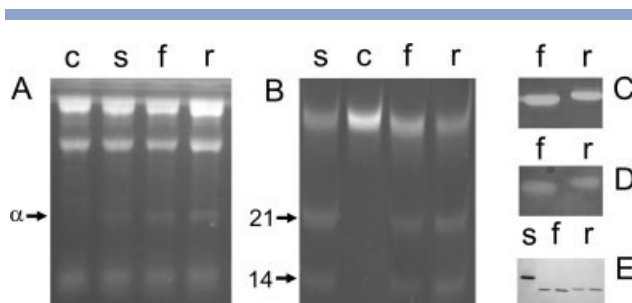
The enzymatic activity of HtA has been analyzed using various substrates: (i) intact ribosomes, (ii) a 35mer oligonucleotide mimicking the sarcin/ricin loop (SRL-RNA), (iii) polymeric nonspecific substrates, poly(C), poly(A), and *Torula* yeast RNA (purified to remove contaminants and small oligonucleotides), and (iv) the dinucleoside phosphates CpC and ApA, which were also used to calculate kinetic parameters.<sup>3,4,23,47-49</sup> HtA (fungal and recombinant forms) produced the 400-nt  $\alpha$ -fragment when assayed against ribosomes from a cell-free reticulocyte lysate, exhibiting the characteristic activity of the  $\alpha$ -sarcin family of proteins [Fig. 5(A)]. Image analysis of the gel revealed that the HtA activity was about two-fold higher than that of  $\alpha$ -sarcin. Both HtA forms degraded the 35mer SRL-RNA; the two bands of the 14mer and 21mer oligonucleotides resulted from the specific hydrolysis of a single phosphodiester bond [Fig. 5(B)]. In this assay, the activity of HtA was quantitatively the same as that of  $\alpha$ -sarcin. HtA produced extensive degradation of *Torula* yeast RNA [Fig. 5(D)]. Neither the fungal nor the recombinant HtA cleaved poly(A), one of the best homopolymer substrates for  $\alpha$ -sarcin, a purine-specific RNase.<sup>2</sup>

**Table I**

Thermodynamic Parameters of the Thermal Denaturation of  $\alpha$ -sarcin and hirsutellin A

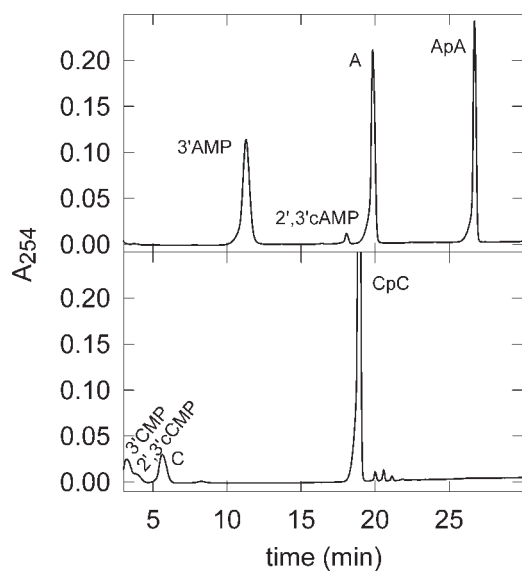
	$\alpha$ -sarcin <sup>41,46</sup>	HtA
$T_m$ (°C) CD measurements	52	62
$\Delta H_m$ (Kcal/mol) CD measurements	142	93
$T_m$ (°C) calorimetric measurements	52.6	61.8
$\Delta H$ (Kcal/mol) calorimetric measurements	136	85

Measurements were performed at pH 7.0, at 30°C/h scan rate.

**Figure 5**

(A) Ribosome-cleaving activity assay of  $\alpha$ -sarcin (s), fungal (f) and recombinant HtA (r), and control in absence of ribotoxin (c). The highly specific ribonuclease activity of the ribotoxins is shown by the release of the 400-nt  $\alpha$ -fragment (arrow  $\alpha$ ) from the 28S rRNA of eukaryotic ribosomes. Cell-free reticulocyte lysates were incubated in the presence of 100 ng of each protein. The reaction mixture was analyzed on 2.4% agarose gels and stained with ethidium bromide. (B) Activity assay on the 35mer oligonucleotide mimicking the sarcin/ricin loop (SRL/RNA). This substrate was incubated in presence of 100 ng of (s)  $\alpha$ -sarcin, (f) fungal and (r) recombinant HtA, (c) control in absence of ribotoxin. The two arrows indicate the position of the 21mer and 14mer oligonucleotides resulting from the specific cleavage of a single phosphodiester bond. (C,D) Zymogram assay of the ribonucleolytic activity against poly(C) and *Torula* yeast RNA, respectively, at pH 7 of 1  $\mu$ g of fungal (f) and recombinant HtA (r). (E) Coomassie-blue stained polyacrylamide gel electrophoresis of proteins: (s)  $\alpha$ -sarcin, (f) fungal and (r) recombinant HtA (two lanes for each one).

However, both HtA forms degraded poly(C), a substrate resistant to degradation by  $\alpha$ -sarcin<sup>2</sup> [Fig. 5(C)]. Dinucleoside phosphates (ApA and CpC) were substrates for both HtA and  $\alpha$ -sarcin (Fig. 6). The catalytic efficiency

**Figure 6**

Ribonuclease activity assay of HtA on dinucleotides. HPLC separation profiles of the reaction products from the cleavage of ApA (A) and CpC (B) obtained by recording the absorbance at 254 nm ( $A_{254nm}$ ). The substrate concentration was 80  $\mu$ M. An enzyme concentration of 4.5  $\mu$ M, incubated for 15 h at room temperature, was used for both assays.

**Table II**  
Kinetic Parameters of the Activities Against ApA and CpC Dinucleoside Phosphates

Protein	Substrate	$K_m$ ( $\mu$ M)	$K_{cat}$ ( $s^{-1}$ )	$K_{cat}/K_m$ ( $M^{-1}s^{-1}$ )
HtA	ApA	32.7	$1.03 \times 10^{-4}$	3.15
HtA	CpC	716	$5.5 \times 10^{-4}$	0.76
$\alpha$ -sarcin <sup>17</sup>	ApA	40.0	$1.0 \times 10^{-4}$	2.5
$\alpha$ -sarcin	CpC	422	$5.1 \times 10^{-5}$	0.12

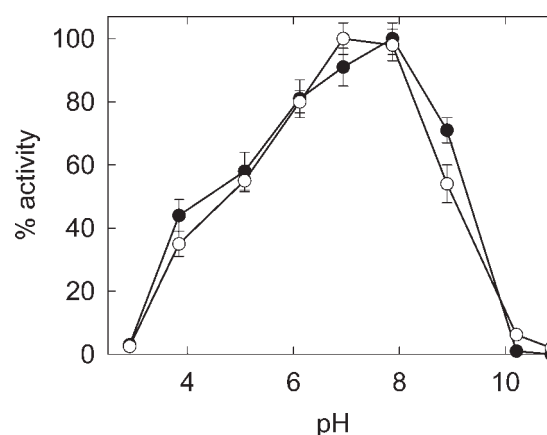
Values determined from the transesterification reaction of dinucleosides by linear regression analysis of double reciprocal plots from three different determinations.

(expressed as the  $K_{cat}/K_m$  ratio) was similar for HtA and  $\alpha$ -sarcin (Table II). Both  $K_{cat}$  and  $K_m$  values were in the same range for ApA, whereas the two  $\alpha$ -sarcin parameters were lower for CpC (Table II). The apparent discrepancy between the results obtained with poly(A) and ApA can be explained by considering the polymeric character of the former substrate and the different assay conditions used. ApA was hydrolyzed in solution, whereas poly(A) was embedded in a polyacrylamide gel.

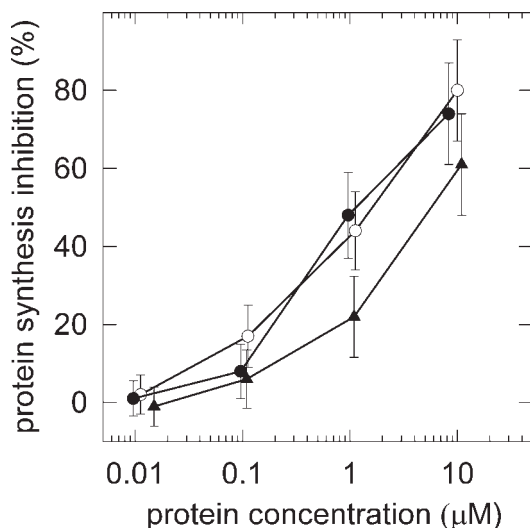
The optimum pH for the degradation of the dinucleoside phosphates ApA and CpC (Fig. 7) is in the range 7–8, although both plots show a shoulder at pH 5.

### Cytotoxic activity

HtA has been reported to be toxic to different mosquito larvae, aphids, and mites.<sup>30,31</sup>  $\alpha$ -Sarcin has been shown to be cytotoxic<sup>5,6,50</sup> for several human tumor cell lines, including RD cells (from human rhabdomyosarcoma). These cells were used to evaluate the potential cytotoxic activity of HtA. Both fungal HtA and  $\alpha$ -sarcin showed almost identical effects ( $IC_{50}$ , 1  $\mu$ M) (Fig. 8) in terms of  $IC_{50}$  (concentration required for 50% protein

**Figure 7**

Effect of pH on the cyclizing ribonuclease activity of HtA on dinucleoside phosphates (ApA, filled circles; CpC open circles). Activity values are expressed as percentages of the maximum value.

**Figure 8**

Protein biosynthesis inhibition promoted by natural and recombinant HtA. Protein biosynthesis inhibition versus concentration of  $\alpha$ -sarcin (solid circles), fungal (open circles) and recombinant HtA (triangles) after 18 h incubation time. The data are expressed as percentages of control samples in the absence of the toxin and are the average  $\pm$  S.D. of three independent experiments with two different samples.

biosynthesis inhibition).<sup>6</sup> Recombinant HtA showed slightly higher  $IC_{50}$  values ( $IC_{50}$ , 5  $\mu$ M), due in part to the presence of the His tail at the  $NH_2$ -terminal end.

### Protein-lipid interaction

It is well known that  $\alpha$ -sarcin interacts with lipid vesicles containing an abundance of acid phospholipids. This interaction results in vesicle aggregation, intermixing of phospholipids from different vesicles (lipid mixing), and leakage of the aqueous contents of its target vesicles.<sup>4,34,40,51</sup> Taking into account the toxic character of HtA, as well as its basic isoelectric point (pI 10.5),<sup>31</sup> its potential interactions with membranes were studied. Vesicle aggregates scatter more light than unaggregated ones, and thus, this process can be analyzed by measuring the resulting apparent absorbance increase at 360 nm of the reaction mixture. In these experiments, HtA did not promote any change in the apparent absorbance at 360 nm [Fig. 9(A)], although different concentrations of protein and neutral (phosphatidylcholine) or acidic (phosphatidylglycerol) phospholipids were used. However, HtA as well as  $\alpha$ -sarcin perturbed the permeability barrier of the phospholipids bilayers as shown in leakage experiments [Fig. 9(B)]. Quantitatively, HtA had a higher membrane-permeabilizing ability than  $\alpha$ -sarcin.

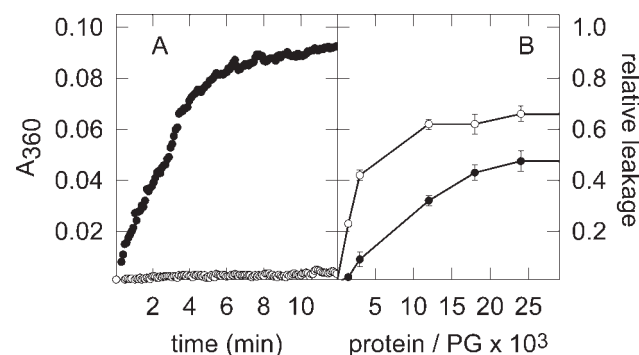
## DISCUSSION

HtA was purified from *Hirsutella thompsonii*<sup>31</sup> and described initially as a mycotoxin displaying ribosome-

inhibiting activity with some specificity to invertebrate cells.<sup>21</sup>  $NH_2$ -terminal sequence analysis of the first 34 amino acid residues did not reveal any significant homology to other known proteins.<sup>21,31</sup> An RNA band of approximately 528 bases was isolated from preparations of Sf-9 insect cells treated with HtA.<sup>21</sup> The internal organelles and cell membranes of these insect cells appeared disrupted upon HtA treatment as revealed by electron microscopy.<sup>21</sup>

Characterization of purified both fungal natural and recombinant HtA did not reveal significant differences in activity and conformation. HtA exhibited ribonuclease activity on dinucleoside phosphates, polymeric RNA substrates, synthetic SRL RNA and ribosomes, being cytotoxic for human tumor cells by inhibiting protein biosynthesis. When using rabbit ribosomes as substrate, it produced the characteristic ribotoxins'  $\alpha$ -fragment. Thus, the first conclusion from these results is that HtA is a member of the  $\alpha$ -sarcin/restrictocin ribotoxin family.

Ribotoxins are an intriguing group of proteins regarding structure-function relationships. Their three-dimensional structure is similar to nontoxic fungal ribonucleases such as RNase T1 to the extent that a common ancestor for both families has been suggested.<sup>19,20</sup> Significantly, nontoxic RNases neither interact with cell membranes nor specifically degrade ribosomes. Ribotoxins and RNase T1-like ribonucleases display a predominance of  $\beta$ -sheet and an irregular secondary structure. Secondary structure analysis of HtA by far-UV CD (Fig. 3) corroborated the abundance of  $\beta$ -conformation in the protein. This fact agrees with the predictions based on the sequence similarity between HtA and  $\alpha$ -sarcin. The fact that these proteins display the same pattern of disulfide bridges and sequence alignment predicts that the

**Figure 9**

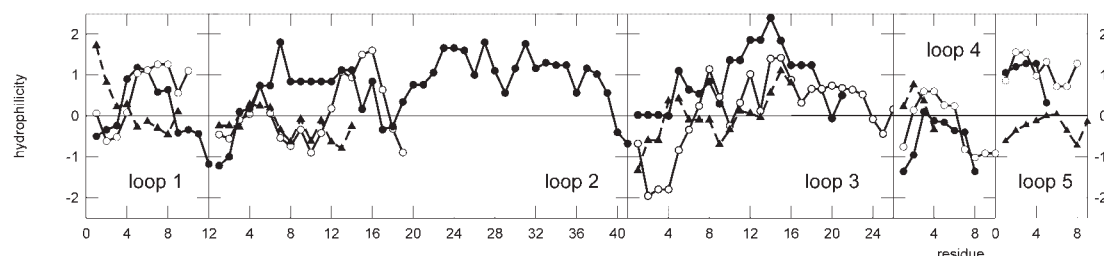
Effect of HtA on phosphatidylglycerol (PG) vesicles. (A) Aggregation of vesicles measured as the increase of absorbance at 360 nm induced by the protein on a vesicle sample ( $A_{360}$  nm versus protein/lipid molar ratio),  $\alpha$ -sarcin (solid circles), natural HtA (open circles). (B) Leakage of intravesicular aqueous contents (relative leakage considering that produced by detergent as unit) versus protein/lipid molar ratio.



**A**

protein	$\beta_1$ -strand	$P_\beta$	$\beta_2$ -strand	$P_\beta$	$\beta_3$ -strand	$P_\beta$	$\beta_4$ -strand	$P_\beta$	$\beta_5$ -strand	$P_\beta$
SAR	50HWF52	1.21	94LLEF97	1.09	120ARVIY124	1.31	133GIIAHT138	1.14	140E--LKL143	0.93
HtA	42HRY44	1.09	64LWEY67	1.13	94IRVVY98	1.48	109GVMTHS114	1.05	123KEFFEK128	0.83

protein	$\alpha$ -helix	$P_\alpha$
SAR	27QNKAESNSHHA37	1.05
HtA	21VATAQAQARKA31	1.21

**B****Figure 10**

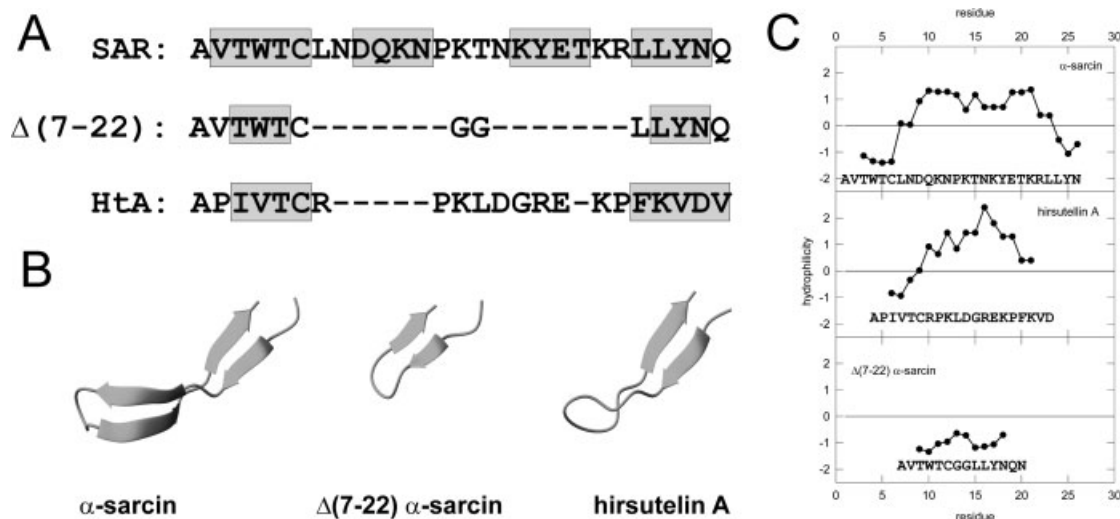
(A) Alignment and structure predictions for the potentially secondary structure ordered regions of HtA. Secondary structure propensities were calculated according to the reference parameters given in Ref. 52.  $P_\alpha$  and  $P_\beta$  are the average propensities for the corresponding regions. (B) Hydrophilicity plots<sup>53</sup> for the loops of  $\alpha$ -sarcin and the corresponding regions of HtA.  $\alpha$ -sarcin (filled circles); HtA (open circles); RNase T1 (triangles).

propensities for  $\alpha$ -helix and  $\beta$ -structures in HtA correspond to those of  $\alpha$ -sarcin [Fig. 10(A)]. The  $\beta$ -structure core of ribotoxins appears to be largely conserved in HtA [Fig. 10(A)]. Four of the  $\beta$ -strands of  $\alpha$ -sarcin ( $\beta_1$  to  $\beta_4$ ) can be easily predicted in HtA. Residues of the single  $\alpha$ -helix of  $\alpha$ -sarcin have an average helical parameter<sup>52</sup> of 1.05, this value being 1.21 for the corresponding aligned region of HtA. Regarding the characteristic  $\text{NH}_2$ -terminal  $\beta$ -hairpin of ribotoxins, HtA displays a shorter sequence at this region, but this structural motif is still present in HtA (Fig. 11). Most of the protein loops of  $\alpha$ -sarcin displayed similar hydrophilicity to the corresponding regions in HtA [Fig. 10(B)]. Only loop 2 of  $\alpha$ -sarcin cannot be recognized in HtA because of the shortening of HtA in this region [Fig. 10(B)].

Ribonuclease and ribotoxin catalyzed reactions occur by an in-line transphosphorylation mechanism involving both base and acid catalysts at either side of the scissile bond. Glu-96 and His-137 of  $\alpha$ -sarcin are the base and acid, respectively<sup>17,55</sup> (Glu-58, and His-92 in RNase T1) (Fig. 1). This mechanism appears to be conserved in HtA, the corresponding counterparts being Glu-66 and His-113, according to the above sequence alignment (Fig. 1). His-50 of  $\alpha$ -sarcin is also involved in catalysis, probably orientating the nucleophile for attack on the phosphorus, and it has a counterpart in HtA, His-42. There are three other residues of RNase T1: Tyr-38, Arg-77, and Phe-100 involved in catalysis; they have been proposed to form a prearranged structural and dielectric microenvironment complementary to the equatorial oxy-

gens of the transition state.<sup>55</sup> The catalytic participation of the corresponding three residues in  $\alpha$ -sarcin, Tyr-48, Arg-121, and Leu-145, has also been demonstrated.<sup>47,51,56</sup> On the basis of these studies and others performed with crystal structures of complexes of the  $\alpha$ -sarcin-like ribotoxin restrictocin with inhibitors,<sup>57</sup> it has been proposed that those residues enable the base flipping performed by His-50/Glu-96/His-137 that permits ribonuclease cleavage at a unique phosphodiester bond. Two of the residues can be easily related to Arg-95 and Phe-126 in HtA based on sequence alignments (Fig. 1). Phe-100 of RNase T1 was substituted in the previously known ribotoxins by Leu-145, but a phenylalanine residue, Phe-126, appears in HtA. Thus, in addition to the specific cleavage performed on ribosomes, the characteristic structural determinants of the ribotoxins were found in HtA despite its shorter sequence (130 residues against 150 for the other ribotoxins). The orientation and proximity of Tyr-44 of HtA suggests its equivalence to the Tyr-48 in  $\alpha$ -sarcin.

The extremely high substrate specificity of  $\alpha$ -sarcin and HtA is due to the existence of regions interacting with SRL.<sup>14,15,58</sup> One of the predicted zones is a lysine-rich region in loop3 ( $\alpha$ -sarcin residues 110–114). This prediction has been confirmed by a deletion mutant of the corresponding loop in the ribotoxin mitogillin that lacks the ability to recognize and cleave the SRL RNA.<sup>20</sup> The putative loop 3 in HtA also possesses a positive charge and hydrophilic properties (Figs. 1 and 10), providing HtA with the specific ribonuclease activity.

**Figure 11**

(A) NH<sub>2</sub>-terminal β-hairpin of ribotoxins: α-sarcin and its Δ(7-22) deletion mutant, and HtA. Residues involved in β-strands are in the grey boxes. (B) Three-dimensional structure of these regions of the three proteins. Diagrams were generated with the MOLMOL program<sup>13</sup> from the atomic coordinates deposited in PDB (entries: 1DE3 and 1R4Y for α-sarcin and its deletion mutant). The atomic coordinates for the corresponding region of HtA were generated with the FUGUE Program<sup>54</sup> at its server (<http://www-cryst.bioc.cam.ac.uk/~fugue/prfsearch.html>). The three structures were fitted to the atomic coordinates of the peptide bonds atoms of residues 5 and 6 of the three proteins (RMSD, 0.221). (C) Hydrophobicity plots<sup>53</sup> of the NH<sub>2</sub>-terminal segment of the three considered proteins.

HtA displayed nonspecific ribonuclease activity against poly(C), as observed for other natural or mutant ribotoxins with identical ribosomal cleavage specificity but showed different specificities when assayed against homopolynucleotides.<sup>59</sup> It has been proposed that the enzymatic efficiency of α-sarcin is dependent on the interactions between the catalytic His-137 residue, loop 5, and the amino-terminal β-hairpin by comparison with the nontoxic RNase T1.<sup>15,60</sup> The catalytic properties of ribotoxins against nonspecific substrates seem to depend on the interaction between residues of the NH<sub>2</sub>-terminal hairpin of these proteins that affects the environment and/or accessibility of His 137.<sup>23</sup> It has been demonstrated that the introduction of either single or deletion mutations in the amino-terminal region gives rise to ribotoxin variants with modified nonspecific ribonucleolytic activity.<sup>19</sup> Therefore, it seems feasible that the putative NH<sub>2</sub>-terminal β-hairpin predicted in HtA (shorter than in other ribotoxins) is responsible for the obtained effect on nonspecific substrates.

The cytotoxic action of α-sarcin can be dissected into three steps: (i) interaction with the target cells and translocation (the ribotoxin is internalized via endocytosis involving acidic endosomes and the Golgi),<sup>4,5</sup> (ii) interaction with the ribosome and specific ribonucleolytic activity, and (iii) cell death by apoptosis as a result of the ribotoxin action. The interaction with the target cell depends on direct molecular interactions between protein and membrane elements because no specific cell receptor has been found for ribotoxins. This step has been widely

studied for α-sarcin, and it is considered to occur initially through electrostatic interaction with acid phospholipids of the membranes, which are more abundant in transformed cells. α-Sarcin produced large alterations of lipid vesicles, including aggregation, lipid mixing, and leakage of intravesicular aqueous contents. HtA also promoted dramatic changes in these vesicles, as have other studied ribotoxins, resulting in leakage of their aqueous contents. These results agree with the observed disruption of cell membranes and organelles in HtA-treated insect cells.<sup>21</sup> As mentioned above, ribotoxins' loops, charged and devoid of ordered secondary structure, are absent in the fungal nontoxic RNases. Considering that these proteins do not interact with phospholipids bilayers, it has been proposed that these loops are largely responsible for the interaction of ribotoxins with membranes. In general, vesicle-interacting proteins can either cause vesicle aggregation or intermixing of lipids from different vesicles between aggregated vesicles with or without leakage of aqueous intravesicular contents, or leakage without vesicle aggregation. Regarding this, HtA and α-sarcin showed a significant difference. α-Sarcin promoted the formation of large lipid vesicles aggregates, while HtA did not (Fig. 9). However, both proteins promote leakage of vesicle contents. Two regions of α-sarcin have been proposed to be specifically involved in vesicle aggregation, loop 2 and the NH<sub>2</sub>-terminal hairpin,<sup>34</sup> regions that are located at opposite ends of the protein molecule. The two main structural differences between HtA and α-sarcin based on the sequence alignment, are

precisely related to these two regions (Figs. 1, 10, and 11). Loop 2 of  $\alpha$ -sarcin is much shorter in HtA (58–68 and 80–92 portions within the 53–93 loop 2 of  $\alpha$ -sarcin are absent), and two of the  $\beta$ -strands of the hairpin are not present in HtA (Figs. 1 and 11). Stopped-flow analysis of vesicle aggregation promoted by  $\alpha$ -sarcin has revealed that the large vesicle aggregates were maintained by essentially electrostatic protein–protein interactions,<sup>34</sup> and the above mentioned  $\alpha$ -sarcin regions are likely to be involved, since their absence in HtA abolishes its capability to aggregate vesicles without disturbing its leakage-inducing activity (Fig. 9).

HtA displayed a higher thermal stability than  $\alpha$ -sarcin, a protein that is less stable than most of the other well-characterized ribotoxins.<sup>10,23</sup>  $\alpha$ -Sarcin is less stable because of the unusual backbone torsional angles of Glu-140, which maintain the unique conformation of loop 5.<sup>15</sup> These angles are maintained by a salt-bridge between Glu-140 and Lys-11, as proved by the fact that a K11L mutant of  $\alpha$ -sarcin displayed an increased thermal stability.<sup>23</sup> The shorter NH<sub>2</sub>-terminal hairpin of HtA precludes the formation of such a bond, thus increasing the  $T_m$  of the protein (62°C of HtA, 59°C of restrictocin, and 52°C of  $\alpha$ -sarcin).

It has been reported that *in vivo* HtA preparations are highly toxic to *Galleria mellonella* larvae<sup>30</sup> and to the adult citrus rust mite, *Phyllocoptruta oleivora*, the natural host of the parasitic fungus *H. thompsonii*.<sup>61</sup> HtA has cytopathic effects on certain insect cell lines such as *Spodoptera frugiperda* cells. HtA also inhibited the Brome mosaic virus protein synthesis *in vitro* translation system.<sup>21</sup> A variety of reports suggest that HtA has broad insecticidal activity, although it has been suggested that the insecticidal activity of filtrates from cultures of *H. thompsonii* was only partially due to HtA production.<sup>62</sup> On the other hand, it is well known that  $\alpha$ -sarcin is cytotoxic to different human tumor cell lines, including rhabdomyosarcoma cells.<sup>5,6</sup> HtA has also shown toxic activity against these cells. This cytotoxic activity may be correlated with its lipid-interacting ability involving a destabilization of the lipid vesicles that modifies membrane permeability. Presumably, this mechanism facilitates the internalization of HtA followed by its ribonucleolytic action on the ribosomes, which results in cell death, most probably by apoptosis.<sup>6</sup>

In summary, it can be concluded that HtA is a ribotoxin of the  $\alpha$ -sarcin-restrictocin family. Its structural and ribonucleolytic characteristics can be explained by the known three-dimensional structures of these two proteins. Our results demonstrate that the characteristic NH<sub>2</sub>-terminal  $\beta$ -hairpin of ribotoxins, which plays an essential role in ribonuclease activity, membrane interaction, and ribosome recognition by ribotoxins, can be shortened as shown with HtA without loss of specificity. The identical conclusion can be extracted regarding loop 2 of ribotoxins, another crucial region for the specific ac-

tivity of these proteins. Ribotoxins are considered to be naturally engineered proteins that evolved from the nontoxic ribonucleases. The results of this study prove that the characteristic abilities of ribotoxins can be accommodated into a shorter amino acid sequence of intermediate size between that of the nontoxic ribonucleases and that of previously known ribotoxins. Clearly, our understanding of the fungal ribotoxins field has grown and points to an intriguing question: is HtA a refined ribotoxin, in which their characteristic functions are accommodated into a shorter polypeptide? Or, on the contrary, may the longer loops of the other ribotoxins have unknown roles?

## REFERENCES

- Schindler GD, Davies JE. Specific cleavage of ribosomal RNA caused by  $\alpha$ -sarcin. *Nucleic Acids Res* 1977;4:1097–1110.
- Endo Y, Hubert PW, Wool IG. The ribonuclease activity of the cytotoxin  $\alpha$ -sarcin: the characteristics of the enzymatic activity of  $\alpha$ -sarcin with ribosomes and ribonucleic acids as substrates. *J Biol Chem* 1983;258:2662–2667.
- Martínez-Ruiz A, García-Ortega L, Kao R, Lacadena J, Oñaderra M, Mancheño JM, Davies J, Martínez del Pozo A, Gavilanes JG. RNase U2 and alpha-sarcin: a study of relationships. *Methods Enzymol* 2001;341:335–351.
- Lacadena J, Álvarez-García E, Carreras-Sangrá N, Herrero-Galán E, Alegre-Cebollada J, García-Ortega L, Oñaderra M, Gavilanes JG, Martínez del Pozo A. Fungal ribotoxins: molecular dissection of a family of natural killers. *FEMS Microbiol Rev* 2007;31:212–237.
- Turnay J, Olmo N, Jiménez J, Lizarbe MA, Gavilanes JG. Isolation and characterization of the ecto-5'-nucleotidase from a rat glioblastoma cell line. *Mol Cell Biochem* 1993;122:39–47.
- Olmo N, Turnay J, González de Buitrago G, López de Silanes I, Gavilanes JG, Lizarbe MA. Cytotoxic mechanism of the ribotoxin alpha-sarcin. Induction of cell death via apoptosis. *Eur J Biochem* 2001;268:2113–2123.
- Parente D, Raucchi G, Celano B, Pacilli A, Zanon L, Canevari S, Adobati E, Colnaghi MI, Dosio F, Arpicco S, Cattell L, Mele A, De Santis R. Clavin, a type-1 ribosome-inactivating protein from *Aspergillus clavatus* IFO 8605. cDNA isolation, heterologous expression, biochemical and biological characterization of the recombinant protein. *Eur J Biochem* 1966;239:272–270.
- Huang KC, Huang Y, Hwu L, Lin A. Characterization of a new ribotoxin gene (c-sar) from *Aspergillus clavatus* (1997). *Toxicon* 1997; 35:383–392.
- Wirth J, Martínez del Pozo A, Mancheño JM, Martínez-Ruiz A, Lacadena J, Oñaderra M, Gavilanes JG. Sequence determination and molecular characterization of gigantins, a cytotoxic protein produced by the mould *Aspergillus giganteus* IFO 5818. *Arch Biochem Biophys* 1997;343:188–193.
- García-Ortega L, Lacadena J, Villalba M, Rodríguez R, Crespo JE, Rodríguez J, Pascual C, Olmo N, Oñaderra M, Martínez del Pozo A, Gavilanes JG. Production and characterization of a noncytotoxic deletion variant of the *Aspergillus fumigatus* allergen Aspfl displaying reduced IgE binding. *FEBS J* 2005;272:2536–2544.
- Martínez-Ruiz A, Kao R, Davies J, Martínez del Pozo A. Ribotoxins are a more widespread group of proteins within the filamentous fungi than previously believed. *Toxicon* 1999;37:1549–1563.
- Martínez-Ruiz A, Martínez del Pozo A, Lacadena J, Oñaderra M, Gavilanes JG. Hirsutellin A displays significant homology to microbial extracellular ribonucleases. *J Invertebr Pathol* 1999;74:96–97.
- Koradi R, Billeter M, Wütrich K. MOLMOL: a program for display and analysis of macromolecular structures. *J Mol Graph* 1996;14: 51–55.

14. Yang X, Moffat K. Insights into specificity of cleavage and mechanism of cell entry from the crystal structure of the highly specific *Aspergillus* ribotoxin, restrictocin. *Structure* 1996;4:837–852.
15. Pérez-Cañadillas JM, Santoro J, Campos-Olivas R, Lacadena J, Martínez del Pozo A, Gavilanes JG, Rico M, Bruix M. The highly refined solution structure of the cytotoxic ribonuclease alpha-sarcin reveals the structural requirements for substrate recognition and ribonucleolytic activity. *J Mol Biol* 2000;299:1061–1073.
16. Pérez-Cañadillas JM, Guenneugues M, Campos-Olivas R, Santoro J, Martínez del Pozo A, Gavilanes JG, Rico M, Bruix M. Backbone dynamics of the cytotoxic ribonuclease alpha-sarcin by 15N NMR relaxation methods. *J Biomol NMR* 2002;24:301–316.
17. Lacadena J, Martínez del Pozo A, Lacadena V, Martínez-Ruiz A, Mancheño JM, Oñaderra M, Gavilanes JG. The cytotoxin alpha-sarcin behaves as a cyclizing ribonuclease. *FEBS Lett* 1998;424:46–48.
18. Lacadena J, Martínez del Pozo A, Martínez-Ruiz A, Pérez-Cañadillas JM, Bruix M, Mancheño JM, Oñaderra M, Gavilanes JG. Role of histidine-50, glutamic acid-96, and histidine-137 in the ribonucleolytic mechanism of the ribotoxin alpha-sarcin. *Proteins* 1999;37:474–484.
19. Lamy B, Davies J, Schindler D. The *Aspergillus* ribonucleolytic toxins (ribotoxins). In: Frankel AE, editor. *Genetically engineered toxins*. New York: Marcel Dekker; 1992. pp 237–258.
20. Kao R, Davies J. Fungal ribotoxins: a family of naturally engineered targeted toxins? *Biochem Cell Biol* 1995;73:1151–1159.
21. Liu JC, Boucias DG, Pendland JC, Liu WZ, Maruniak J. The mode of action of hirsutellin A on eukaryotic cells. *J Invertebr Pathol* 1996;67:224–228.
22. Boucias DG, Farmerie WG, Pendland JC. Cloning and sequencing of cDNA of the insecticidal toxin hirsutellin A. *J Invertebr Pathol* 1998;72:258–261.
23. García-Ortega L, Lacadena J, Mancheño JM, Oñaderra M, Kao R, Davies J, Olmo N, Martínez del Pozo A, Gavilanes JG. Involvement of the amino-terminal beta-hairpin of the *Aspergillus* ribotoxins on the interaction with membranes and nonspecific ribonuclease activity. *Protein Sci* 2001;10:1658–1668.
24. García-Ortega L, Masip M, Mancheño JM, Oñaderra M, Lizarbe MA, García Mayoral MF, Bruix M, Martínez del Pozo A, Gavilanes JG. Deletion of the NH2-terminal beta-hairpin of the ribotoxin alpha-sarcin produces a nontoxic but active ribonuclease. *J Biol Chem* 2002;277:18632–18639.
25. Rodríguez-Crespo I, Gerber NC, Ortiz de Montellano PR. Endothelial nitric-oxide synthase. Expression in *Escherichia coli*, spectroscopic characterization, and role of tetrahydrobiopterin in dimer formation. *J Biol Chem* 1996;271:11462–11467.
26. Cook S, Galve-Roperh I, Martínez del Pozo A, Rodríguez-Crespo I. Direct calcium binding results in activation of brain serine racemase. *J Biol Chem* 2002;277:27782–27792.
27. Lacadena J, Martínez del Pozo A, Barbero JL, Mancheño JM, Gasset M, Oñaderra M, López-Otín C, Ortega S, García J, Gavilanes JG. Overproduction and purification of biologically active native fungal alpha-sarcin in *Escherichia coli*. *Gene* 1994;142:147–151.
28. De los Ríos V, Oñaderra M, Martínez-Ruiz A, Lacadena J, Mancheño JM, Martínez del Pozo A, Gavilanes JG. Overproduction in *Escherichia coli* and purification of the hemolytic protein sticholysin II from the sea anemone *Stichodactyla helianthus*. *Protein Expr Purif* 2000;18:71–76.
29. Sambrook J, Russell DW. *Molecular cloning. A laboratory manual*. Cold Spring Harbor, New York: Cold Spring Harbor Laboratory Press; 2001.
30. Liu WZ, Boucias DG, McCoy C. Extraction and characterization of the insecticidal toxin hirsutellin A produced by *Hirsutella thompsonii* var. *thompsonii*. *Exp Mycol* 1995;19:254–262.
31. Mazet I, Vey A. Hirsutellin A, a toxic protein produced *in vitro* by *Hirsutella thompsonii*. *Microbiology* 1995;141:1343–1348.
32. Gasset M, Oñaderra M, Goormaghtigh E, Gavilanes JG. Acid phospholipid vesicles produce conformational changes on the antitumour protein alpha-sarcin. *Biochim Biophys Acta* 1991;1080:51–58.
33. Kao R, Martínez-Ruiz A, Martínez del Pozo A, Crameri R, Davies J. Mitogillin and related fungal ribotoxins. *Methods Enzymol* 2001;341:324–335.
34. Mancheño JM, Gasset M, Lacadena J, Ramón F, Martínez del Pozo A, Oñaderra M, Gavilanes JG. Kinetic study of the aggregation and lipid mixing produced by alpha-sarcin on phosphatidylglycerol and phosphatidylserine vesicles: stopped-flow light scattering and fluorescence energy transfer measurements. *Biophys J* 1994;67:1117–1125.
35. Barlett GR. Colorimetric assay methods for free and phosphorylated glyceric acids. *J Biol Chem* 1959;234:466–468.
36. Gasset M, Martínez del Pozo A, Oñaderra M, Gavilanes JG. Study of the interaction between the antitumour protein alpha-sarcin and phospholipid vesicles. *Biochem J* 1989;258:569–575.
37. Mancheño JM, Martínez del Pozo A, Albar JP, Oñaderra M, Gavilanes JG. A peptide of nine amino acid residues from alpha-sarcin cytotoxin is a membrane-perturbing structure. *J Peptide Res* 1998;51:142–148.
38. Gasset M, Oñaderra M, Thomas PG, Gavilanes JG. Fusion of phospholipid vesicles produced by the anti-tumour protein alpha-sarcin. *Biochem J* 1990;265:815–822.
39. Gasset M, Oñaderra M, Martínez del Pozo A, Schiavo GP, Laynez J, Usobiaga P, Gavilanes JG. Effect of the antitumour protein alpha-sarcin on the thermotropic behaviour of acid phospholipid vesicles. *Biochim Biophys Acta* 1991;1068:9–16.
40. Gasset M, Mancheño JM, Lacadena J, Turnay J, Olmo N, Lizarbe MA, Martínez del Pozo A, Oñaderra M, Gavilanes JG. Alpha-sarcin, a ribosome-inactivating protein that translocates across the membrane of phospholipids vesicles. *Curr Topics Peptide Prot Res* 1994;1:99–104.
41. Gasset M, Mancheño JM, Laynez J, Lacadena J, Fernández-Ballester G, Martínez del Pozo A, Oñaderra M, and Gavilanes JG. Thermal unfolding of the cytotoxin alpha-sarcin: phospholipid binding induces destabilization of the protein structure. *Biochim Biophys Acta* 1995;1252:126–134.
42. Oñaderra M, Mancheño JM, Gasset M, Lacadena J, Schiavo G, Martínez del Pozo A, Gavilanes JG. Translocation of alpha-sarcin across the lipid bilayer of asolectin vesicles. *Biochem J* 1993;295:221–225.
43. Mancheño JM, Gasset M, Albar JP, Lacadena J, Martínez del Pozo A, Oñaderra M, Gavilanes JG. Membrane interaction of a beta-structure-forming synthetic peptide comprising the 116–139th sequence region of the cytotoxic protein alpha-sarcin. *Biophys J* 1995;68:2387–2395.
44. Pace CN, Vajdos F, Fee L, Grimsley G, Gray T. How to measure and predict the molar absorption coefficient of a protein. *Protein Sci* 1995;4:2411–2423.
45. Perczel A, Hollosi M, Tusnady G, Fasman GD. Convex constraint analysis: a natural deconvolution of circular dichroism curves of proteins. *Protein Eng* 1991;4:669–679.
46. de Antonio C, Martínez del Pozo A, Mancheño JM, Oñaderra M, Lacadena J, Martínez-Ruiz A, Pérez-Cañadillas JM, Bruix M, Gavilanes JG. Assignment of the contribution of the tryptophan residues to the spectroscopic and functional properties of the ribotoxin alpha-sarcin. *Proteins* 2000;41:350–361.
47. Masip M, García-Ortega L, Olmo N, García-Mayoral MF, Pérez-Cañadillas JM, Bruix M, Oñaderra M, Martínez del Pozo A, Gavilanes JG. Leucine 145 of the ribotoxin alpha-sarcin plays a key role for determining the specificity of the ribosome-inactivating activity of the protein. *Protein Sci* 2003;12:161–169.
48. Siemer A, Masip M, Carreras N, García-Ortega L, Oñaderra M, Bruix M, Martínez del Pozo A, Gavilanes JG. Conserved asparagine residue 54 of alpha-sarcin plays a role in protein stability and enzyme activity. *Biol Chem* 2004;385:1165–1170.
49. García-Segura JM, Orozco MM, Fominaya JM, Gavilanes JG. Purification, molecular and enzymic characterization of an acid RNase from the insect *Ceratitis capitata*. *Eur J Biochem* 1986;158:367–372.



50. Olson BH, Jennings JC, Roga V, Junek AJ, Schuurmans DM. Alpha-sarcin, a new antitumor agent. II. Fermentation and antitumor spectrum. *Appl Microbiol* 1965;13:322–326.
51. Masip M, Lacadena J, Mancheño JM, Oñaderra M, Martínez-Ruiz A, Martínez del Pozo A, Gavilanes JG. Arginine 121 is a crucial residue for the specific cytotoxic activity of the ribotoxin alpha-sarcin. *Eur J Biochem* 2001;268:6190–6196.
52. Chou PY, Fasman GD. Empirical predictions of protein conformation. *Annu Rev Biochem* 1978;47:231–276.
53. Hopp TP, Woods KR. Prediction of protein antigenic determinants from amino acid sequences. *Proc Natl Acad Sci USA* 1981;78:3824–3828.
54. Shi J, Blundell TL, Mizuguchi K. FUGUE: sequence-structure homology recognition using environment-specific substitution tables and structure-dependent gap penalties. *J Mol Biol* 2001;310:243–257.
55. Loverix S, Steyaert J. Deciphering the mechanism of RNase T1. *Methods Enzymol* 2001;341:305–323.
56. Álvarez-García E, García-Ortega L, Verdún Y, Bruix M, Martínez del Pozo A, Gavilanes JG. Tyr-48, a conserved residue in ribotoxins, is involved in the RNA-degrading activity of alpha-sarcin. *Biol Chem* 2006;387:535–541.
57. Yang X, Gerczei T, Glover LT, Correll CC. Crystal structures of restrictocin-inhibitor complexes with implications for RNA recognition and base flipping. *Nat Struct Biol* 2001;8:968–973.
58. Correll CC, Munishkin A, Chan YL, Ren Z, Wool IG, Steitz TA. Crystal structure of the ribosomal RNA domain essential for binding elongation factors. *Proc Natl Acad Sci USA* 1998;95:13436–13441.
59. Fando JL, Alaba I, Escarmis C, Fernández-Luna JL, Méndez E, Salinas M. The mode of action of restrictocin and mitogillin on eukaryotic ribosomes. Inhibition of brain protein synthesis, cleavage and sequence of the ribosomal RNA fragment. *Eur J Biochem* 1985;149:29–34.
60. Pace CN, Heinemann U, Hahn U, Saenger W. Ribonuclease T1: structure, function and stability. *Angew Chem* 1991;30:343–360.
61. Omoto C, McCoy CW. Toxicity of purified fungal toxin hirsutellin A to the citrus rust mite *Phyllocoptruta oleivora* (Ash.). *J Invert Pathol* 1998;72:319–322.
62. Maimala S, Tartar A, Boucias D, Chandrapatya A. Detection of the toxin Hirsutellin A from *Hirsutella thompsonii*. *J Invert Pathol* 2002;80:112–126.